ARTICLE
Journal of Cellular Biochemistry 112:3246–3255 (2011)

Journal of Cellular Biochemistry

HDAC Inhibition Promotes Cardiogenesis and the Survival of Embryonic Stem Cells Through Proteasome-Dependent Pathway

Hong P. Chen,[1] Megan DeNicola,[1] Xin Qin,[1] Yu Zhao,[1] Ling Zhang,[2] Xi L. Long,[3] Shougang Zhuang,[2] Paul Y. Liu,[1] and Ting C. Zhao[1*†]

[1]*Department of Surgery, Roger William Medical Center, Boston University Medical School, Providence, Rhode Island*
[2]*Department of Medicine, Rhode Island Hospital, Brown Medical School, Brown University, Providence, Rhode Island*
[3]*Biomolecular Science Center, University of Central Florida, Orlando, Florida*

ABSTRACT

Histone deacetylase (HDAC) inhibition plays a crucial role in mediating cardiogenesis and myocardial protection, whereas HDAC degradation has recently attracted attention in mediating the biological function of HDACs. However, it remains unknown whether HDAC inhibition modulates cardiogenesis and embryonic stem cell (ESC) survival through the proteasome pathway. Using the well-established mouse ESC culture, we demonstrated that HDAC inhibitors, both trichostatin A (TSA,50 nmol/L) and sodium butyrate (NaB, 200 μmol/L) that causes the pronounced reduction of HDAC4 activity, decreased cell death and increased viability of ESCs in response to oxidant stress. HDAC inhibition reduced the cleaved caspases 3, 6, 9, PARP, and TUNEL positive ESCs, which were abrogated with MG132 (0.5 μmol/L), a specific proteasome inhibitor. Furthermore, HDAC inhibition stimulates the growth of embryoid bodies (EB), which are associated with a faster spontaneous rhythmic contraction. HDAC inhibition increases the up-regulation of GATA4, MEF2C, Nkx2.5, cardiac actin, and α-SMA mRNA and protein levels that were abrogated by MG132. TSA and NaB resulted in a significant increase in cardiac lineage commitments that were blocked by the proteasome inhibition. Notably, HDAC inhibitors led to noticeable HDAC4 degradation, which was effectively prevented by MG132. Luciferase assay demonstrates an activation of MEF2 cardiac transcriptional factor by HDAC inhibition, which was repressed by MG132, revealing that the degradation of HDAC4 allows for the activation of MEF2. Taken together, our study is the first to demonstrate that HDAC inhibition through proteasome pathway forms a novel signaling to determine the cardiac lineage commitment and elicits the survival pathway. J. Cell. Biochem. 112: 3246–3255, 2011. © 2011 Wiley Periodicals, Inc.

KEY WORDS: HDAC; PROTEASOME SYSTEM, STEM CELL; CARDIOGENESIS; SURVIVAL

Histone acetyltransferases (HATs) and histone deacetylases (HDACs) have recently garnered attention because they emerged as important mechanisms in the regulation of a variety of cellular responses. Histone acetylation is mediated by HAT, which results in the modification of the structure of chromatin leading to nucleosomal relaxation and altered transcriptional activation. In contrast, the reverse reaction is mediated by HDAC inducing deacetylation, chromatin condensation, and transcriptional repression [Luger et al., 1997; Hansen et al., 1998; Cheung et al., 2000; Strahl and Allis, 2000; Turner, 2000]. The opposing actions of HAT and HDACs allow for gene expression to be exquisitely regulated through chromatin remodeling.

Since the identification of HDAC 1 (named HD 1) [Hassig et al., 1998], 18 HDACs have been characterized in mammals [Verdin et al., 2003]. These HDACs can be categorized into three distinct classes. Class I HDACs consist of HDACs 1, 2, 3, and 8, which are

Conflict of interest: None

[†]Associate Professor

Additional supporting information may be found in the online version of this article.

Grant sponsor: National Heart, Lung, and Blood Institute; Grant number: R01 HL089405; Grant sponsor: American Heart Association-National center; Grant number: 0735458N.

*Correspondence to: T.C. Zhao, MD, Department of Surgery, Roger William Medical Center, Boston University Medical School, 50 Maude Street, Providence, RI 02908. E-mail: tzhao@bu.edu

Received 23 June 2011; Accepted 27 June 2011 • DOI 10.1002/jcb.23251 • © 2011 Wiley Periodicals, Inc.
Published online 12 July 2011 in Wiley Online Library (wileyonlinelibrary.com).

ubiquitously expressed and predominantly located in the nuclei. Class II HDACs include HDAC 4, 5, 7 and 9. In contrast to class I, class II HDACs exhibit a tissue specific pattern of expression. HDAC 4 and HDAC 5 are highly expressed in the heart, brain, and skeletal muscles and shuttle between the nucleus and cytoplasm [Fischle et al., 1999; Grozinger et al., 1999; Wang et al., 1999]. Class III HDACs were identified on the basis of sequence similarity with Sir, a yeast transcriptional repressor that requires the cofactor NDA^{+} for its deacetylase activity (Vigushi and Coombes, 2004). We and others have recently demonstrated that inhibition of HDAC elicited a cardioprotective effect and antagonized cardiac hypertrophy response [Kee et al., 2006; Kong et al., 2006; Zhao et al., 2007].

Mouse genetics have demonstrated an essential role of HDAC in embryogenesis [Lagger et al., 2002; Rusty et al., 2007; Dovey et al., 2010; Foster et al., 2010] and also many HDAC components of HDAC complexes. Germ-line deletion of HDAC1 results in early embryonic lethality around embryonic day (e) 10.5. In contrast to these early embryonic phenotypes, constitutive HDAC4 and HDAC5 knockout mice survive embryogenesis to adulthood and develop severe cardiac hypertrophy in response to hypertrophic stimuli [Zhang et al., 2002; Trivedi et al., 2007]. It has been proposed that an epigenetic event may be rate-limiting in the derivation of new embryonic stem cells (ESCs) [Thomson et al., 1998; Smith, 2001] and may further operate in selecting for ESCs that adapt to standard culture conditions. Consistent with these observations is the recent demonstration that efficiency of iPS cell formation was enhanced upon addition of valproic acid, a HDAC inhibitor [Huangfu et al., 2008]. It is intriguing that ESC can extensively self-renew in response to butyrate, without the need for feeder conditioning or recombinant growth factor, pointing to the existence of a core machinery for ESC self-renewal that is under HDAC control and that can be activated upon HDAC inhibition [Ware et al., 2009; Yuan et al., 2011]. Recent advances have recognized the proteasome pathway as a pivotal mechanism for controlling basic cellular processes such as the cell cycle, differentiation, transcription, and maintenance of cellular quality control [Su and Wang, 2010]. HDAC4 and HDAC5 were recently reported to activate MURF1 E3 ligase to mediate neurogenic muscle atrophy [Moresi et al., 2010]. An earlier study shows that HDAC5 was targeted by the proteasome system in muscles [Potthoff et al., 2007], implying that post-translational modification of HDACs is one of the important mechanisms for the regulation of the biological role of HDACs. It remains unknown whether the proteasome pathway through mediating HDAC degradation governs the self-renewal and cardiac differentiation of ESCs. The ability of ESCs to differentiate into specific cell types holds great potential for therapeutic use in cell therapy. In particular, it will be interesting to identify whether HDAC inhibition through the proteasome pathway facilitates cardiac specification, which would provide further insight into the mechanisms that control cellular plasticity and make it possible to determine the differentiation of ESCs into cardiac tissues. Here, we have fully characterized that HDAC inhibitors stimulate HDAC4 degradation through the proteasome system, which allows for activation of MEF2 that are capable of facilitating the adaptation of ESCs into cardiac decision.

MATERIALS AND METHODS

CHEMICAL SUPPLIES AND ANTIBODIES

Trichostatin A was obtained from Calbiochem (San Diego, CA). MG132, Sodium butyrate, monoclonal anti-smooth muscle actin, monoclonal anti-actinin, leukemia inhibitory factor (LIF), and protease inhibitor cocktail were purchased from Sigma (St. Louis, MO). HDAC 4 polyclonal antibody and apoptosis antibody sampler kits were purchased from Cell Signaling^{Tm} (New England, MA). Nkx2.5, β-actin, MEF2C, GATA4 rabbit polyclonal antibodies were obtained from Santa Cruz Biotechnology (Santa Cruz, CA). The anti-rabbit HRP antibody was purchased from Amersham (Hercules, CA). The goat anti-mouse HRP antibody and trizol reagent were purchased from Invitrogen (Carlsbad, CA). LDH cytotoxicity detection kit was purchased from Clontech (Mountain View, CA). Non-essential amino acids, penicillin, streptomycin, l-glutamine, β-mercaptoethanol, sodium pyruvate, DMEM, and fetal bovine serum were purchased from Hyclone, CGR8 ESCs were obtained from HyperCLDB (UK).

EMBRYONIC STEM CELLS CULTURE

Mouse ESCs (CGR8, generation 12–14) were used in this study. Stem cells were cultivated in gelatin-coated petri-dishes in ESC culture medium consisting of DMEM, $1\times$ non-essential amino acids, 100 μg/ml penicillin, 100 U/ml streptomycin, 2 mmol/L l-glutamine, 0.1 mmol/L β-mercaptoethanol, 1 mmol/L sodium pyruvate, 15% fetal bovine serum, and 10^3 U/ml LIF. Cells were maintained at 37°C in a humidified atmosphere of 5% CO_2. Monolayers were passed by trypsinization at 70%–80% confluence.

IN VITRO DIFFERENTIATION

The "hanging drop" method [Maltsev et al., 1994] was used to induce ESC differentiation [Maltsev et al., 1994]. CGR8 ESCs were dissociated by 0.25% trypsin–0.01% EDTA and re-suspended in the differentiation medium (i.e., ESC medium without LIF). Cell drops (400 cells/20 μl) were placed onto the lids of culture dishes for 2 days to form embryonic bodies (EBs). EBs were then transferred to bacteriological dishes for 5 days. Some of the EBs were further cultured in bacteriological dishes for 7 days. The rest of the EBs were cultured in gelatin-coated 6-well culture plates (8–10 EBs/well). On day 8 of differentiation, the EBs received treatments as follows: 1) Control; 2) TSA (50 nmol/L); 3) Sodium butyrate (NaB, 0.2 mmol/L); 4) MG132 (0.5 μmol/L), 5) TSA + MG132; and 6) NaB + MG132. The medium containing these individual treatments was changed daily. The EB growth was monitored on days 8, 10, 12, and 14 of EB differentiation. Spontaneous rhythmic contraction of EB was assessed under microscopy and measured daily starting from day 9 continuing to 14 of differentiation. The beating rates of EBs were expressed as beats per minutes and determined on day 14 [Maltsev et al., 1994].

CELLULAR OXIDATIVE STRESS, CELL VIABILITY ASSAY AND CYTOTOXICITY ASSAY

ESCs were plated into 6-well plates (5×10^5 cells/well) in differentiation medium overnight. ESCs were plated onto coverslips coated with 0.1% polylysine. The cells were further cultured in

differentiation medium for 24 h. The ESCs were pretreated for 1 h with: 1) Control; 2) TSA (50 nmol/L); 3) NaB (0.2 mmol/L); 4) MG132 (0.5 μmol/L), 5) TSA + MG132; and 6) NaB + MG132 before ESCs were exposed to 100 μmol/L hydrogen peroxide for 2 h and resumed with differentiation medium for 1 h. Finally, cytotoxicity and cell viability were measured according to manufacturers' instructions with minor modifications and expressed as percentage (%) change of LDH to measure cytotoxicity [Zhang et al., 2010].

WESTERN BLOT ANALYSIS

The ESCs were lysed with RIPA buffer (150 mM sodium chloride, 1.0% NP-40, 0.5% sodium deoxycholate, 0.1% SDS, 50 mM Tris, pH 8.0), supplemented with protease inhibitor cocktail. The proteins were detected including anti-α-smooth muscle actin, anti-α-actinin monoclonal antibodies; Nkx2.5, GATA4, MEF2C, and beta-actin rabbit polyclonal antibodies and Apoptosis Antibody Sampler Kit (mouse specific, cleaved caspase-3, 6, 9, and PARP). Proteins (30 μg/lane) were separated by 7% (HDAC 4) and 10% SDS–PAGE for others. The proteins were then transferred onto a nitrocellulose membrane. The membrane was blocked with 5% non-fat dry milk in PBS containing 0.5% Tween 20 for 1 h. The blots were incubated with their respective primary antibodies (1:1,000) overnight at 4°C and visualized by incubation with anti-rabbit or anti-mouse horseradish peroxidase-conjugated antibodies (1:5,000 dilution) for 1 h. The immunoblots were developed with ECL Chemiluminescence Detection Reagent (GE Healthcare, Piscataway, NJ). The densitometric results were normalized to the control group and expressed as percentages of control values.

IMMUNOFLUORESCENT STAINING

On day 14 of ESC differentiation, cultured EBs in suspension were fixed in 4% paraformaldehyde for immunocytochemical analysis using rabbit anti-GATA4, MEF2C or Nkx2.5 (diluted 1:200) for myocyte; mouse anti-α-SMA for mouse smooth muscle actin. A secondary antibody, FITC linked anti-rabbit IgG (1:200) was applied for 1 h at room temperature. Coverslips were counterstained with 4′, 6-diamidino-2-phenylindole (DAPI) to visualize the nuclei. The images were captured with a Zeiss Axiovert 200 fluorescence microscope. Another set of experiments were carried out to determine the percentage of each positive staining in the differentiated cells. The EBs were digested into single cells and plated onto coverslips coated with 0.1% polylysine overnight to evaluate the positive staining described above. The percentage of positive nuclei was normalized with the total number of stained nuclei [Tseng et al., 2010].

REVERSE TRANSCRIPTION POLYMERASE REACTION (RT-PCR)

Total cellular RNA was isolated from the treated EBs (day 14) with Trizol reagent. RNA (5 μg) was reversely transcribed to generate cDNA using standard methodology [Zhao et al., 2001]. The reverse transcribed cDNA (5 μl) was amplified to a final volume of 50 μl by PCR under standard conditions. Based on the sequence for murine cardiac actin, GATA4, MEF2C, Nkx2.5, α-SMA, and GAPDH cDNA, the primers were synthesized with the sequences shown below [Tamaki et al., 2008]. The experimental conditions for PCR were 40 cycles and GAPDH (30 cycles) for 60 s at 94, 55, and 72°C, respectively. After amplification, 10 μl of PCR product per lane was loaded on a 2.0% agarose gel containing ethidium bromide in 0.5 × TBE buffer. The separated PCR products were visualized under ultraviolet (UV) light, and the integrated optical density was determined for each PCR product using AlphaImagerTM 2200. Primers used for each specific product are as follows: Cardiac actin: Forward: 5-TAC CCT GGT ATT GCC GAT CGT-3, Reverse: 5-ACA TCT CAG AAG CAC TTG CGG T-3; GATA4: Forward: 5-TGGGACTTTCTCCAGCACAGA-3, Reverse: 5-CAATGTTAACGGGT-TGTGGAGG -3; MEF2C: Forward: 5-CAC GCC TGT CAC CTA ACA TCC-3, Reverse: 5-TGT TAGCTC TCA AAC GCC ACA C-3; Nkx2.5: Forward: 5-TGT CTC GGA CCT GGC AGA GC-3, Reverse: 5-GGC GAC GGC AAG AC A AC C AG-3; α-SMA: Forward: 5-GCA AAC AGG AAT ACG ACG AAG C-3, Reverse: 5-GCT TTG GGC AGG AAT GAT TTG-3; GAPDH: Forward: 5-ACC ACA GTC CAT GCC ATC AC-3, Reverse: 5-TCC ACC ACC CTG TTG CTG TA-3.

MEASUREMENT OF EB DIAMETER

The suspension EBs that were treated on days 8, 10, 12 and 14 were photographed, and the diameters were measured using image J (Image J software, NIH).

LUCIFERASE ACTIVITY ASSAY

MEF2 luciferase reporter (4X-MEF2-luc) activity assays were described with modification [Zhang et al., 2010]; the differentiated ESCs at 70–80% confluences were transiently transfected with luciferase reporter construct MEF2 4×-Luc or empty vector by the Lipofectamine™ 2000 method (Invitrogen). Twenty-four hours after transfection, cells were treated with TSA, sodium butyrate with or without MG132 at the concentrations described above. Cell lysates were generated and luciferase activity was determined according to the manufacturer's instructions by using the Luciferase Assay System (BioVision Inc). Luciferase activities were measured with TD-20/20 Luminometer (Turner Designs Instrument) five times and results were normalized to the basal levels of the empty vector group.

MEASUREMENT OF HDAC ACTIVITY OF ESCs

To determine effects of HDAC inhibitors on HDAC activity, HDAC activity ESCs after 1-h treatments with HDAC inhibitors and MG132 was measured using the colorimetric HDAC activity assay kit (BioVision Research, Mountain View, CA).

STATISTICS

The results are expressed as the mean± SEM. Differences among the groups were analyzed by one-way analysis of variance (ANOVA), followed by Bonferroni's correction. Statistical differences were considered significant with a value of $P < 0.05$.

RESULTS

HDAC INHIBITION PROTECTS ESC FROM OXIDATIVE STRESS THAT REQUIRES PROTEASOME SYSTEM

In order to examine whether HDAC inhibition prevents ESCs from oxidant injury, ESCs were subjected to oxidant stress. Loss of plasma membrane integrity (cell necrosis) was assessed by measurement of

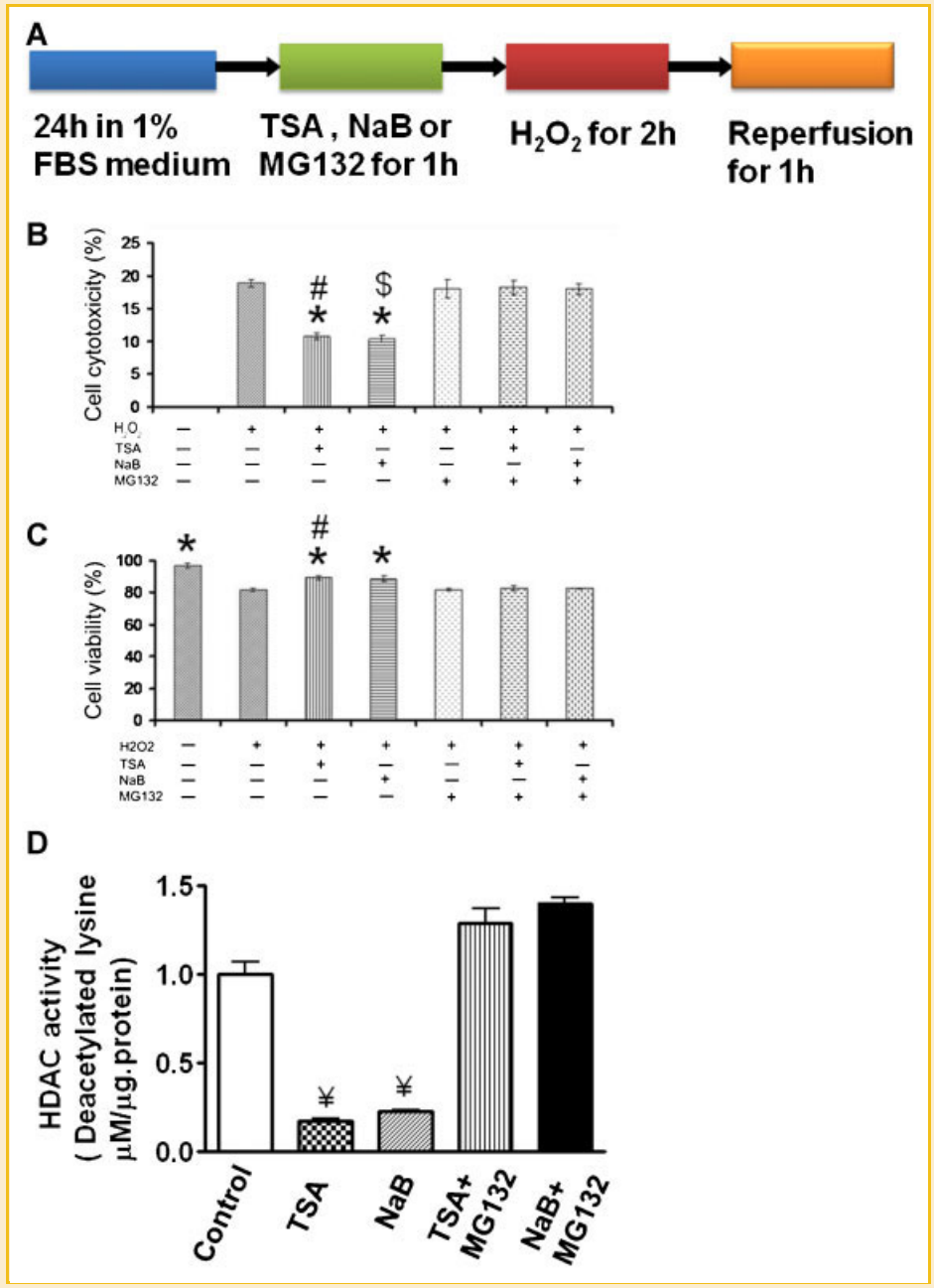

Fig. 1. A: Experimental protocol: See methods for the list of groups and treatments; (B) the LDH release of ESC in culture medium after reperfusion (n = 4 per group); (C) cell viability was measured and quantified (n = 3 per group); ESCs were exposed to oxidant stress (100 μmol/L H_2O_2); a description of oxidant stress is provided under methods; (D) HDAC activities were measured ESCs that were treated with HDAC inhibitors with or without proteasome inhibitor (n = 5 per group).Values represent mean ± SEM; HDAC inhibitor, trichostatin A (50 nmol/L), sodium butyrate (200 μmol/L), MG132 (0.5 μmol/L) were maintained in culture medium. $^{*}P < 0.05$ versus H_2O_2 group, $^{\#}P < 0.05$ versus TSA + MG132, $^{\$}P < 0.05$ versus NaB + MG132 group; $^{¥}P < 0.001$ versus the control group, TSA + MG132 & NaB + MG132.

the activity of lactate dehydrogenase (LDH) in the supernatant. As shown in Figure 1B, LDH release from ESCs in the H_2O_2-treated group was measured at 18.9%, which was reduced to 10.7 and 10.3% by TSA and NaB, respectively, suggesting that the cytotoxicity elicited by H_2O_2 was effectively mitigated by HDAC inhibition ($P < 0.01$). In contrast, the reductions of LDH by TSA and NaB were completely abrogated by MG132, which yielded values of 18.3 and 18%, respectively ($P < 0.01$). In order to examine cell viability in response to oxidant stress, we used trypan blue staining to estimate cell viability. As shown in Figure 1C, cell viability in the control group is 96.7%, which dramatically decreased to 81.6% in the presence of H_2O_2 stimulation. As compared to that of the H_2O_2-treated group, TSA or NaB significantly improved the numbers of viable ESCs ($P < 0.05$), but the effect on viability was eliminated by pretreatment of MG132, a proteasome inhibitor ($P < 0.05$). HDAC activities were significantly inhibited in ESCs treated with

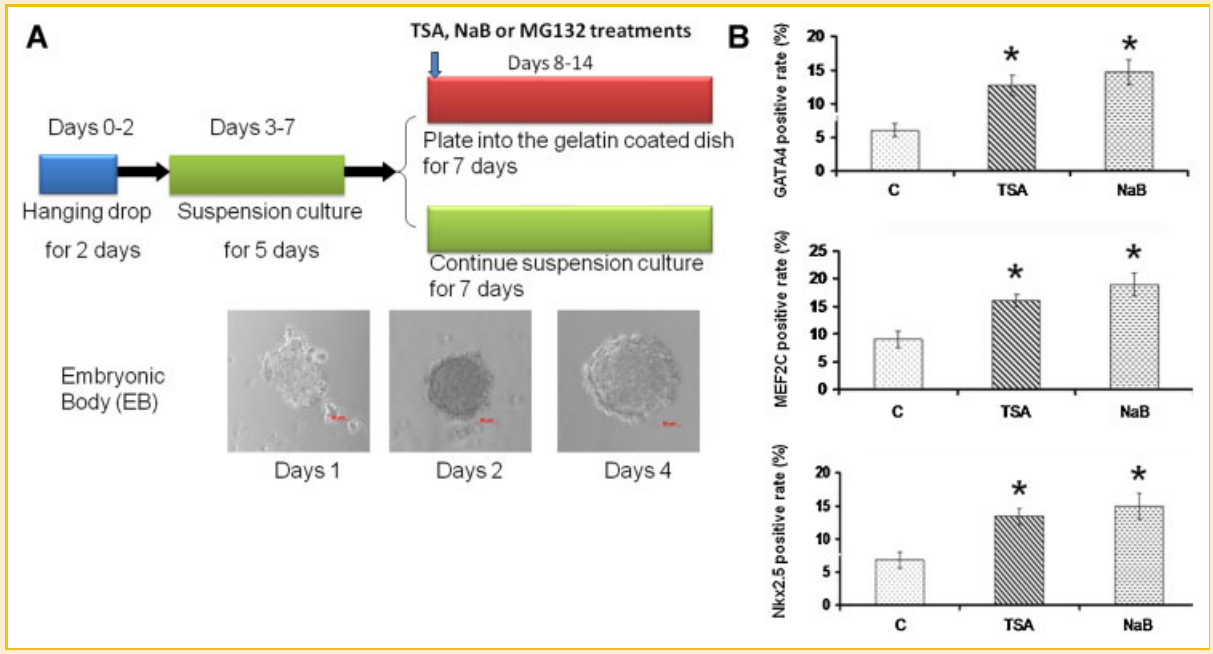

Fig. 2. A: Differentiation experimental protocol: See Methods for the list of groups and treatments; (B) quantification analysis of effect of TSA and NaB on GATA4 positive, MEF2C positive, Nkx2.5 positive staining cells, respectively($n = 3$ per group). Values represent mean ± SEM; $^*P < 0.05$ versus control group; C: control.

trichostatin A and sodium butyrate as compared to the control group, which was abrogated by MG132 (Fig. 1D). In addition, we evaluated ESC morphology under the influence of oxidative stress. Treatments with H_2O_2 displayed poor ESC morphology, while ESC shape was preserved by pretreatment with TSA or NaB. These results indicate that HDAC inhibition protects ESC from oxidant stress injury, which relies on the proteasome system.

We next analyzed the effects of HDAC inhibition on ESC apoptosis. Apoptosis was measured by TUNEL staining. As shown in Supplementary Figure 1, abundant apoptotic positive stainings were demonstrated in ESCs that were exposed to oxidant stress. However, both TSA and NaB significantly reduced the numbers of apoptotic positive stainings, but such an anti-apoptotic effect was abrogated by treatment with MG132. Furthermore, we validated the effect of HDAC inhibitors on the specific apoptotic signaling in ESCs. As illustrated in Supplementary Figure 2, both TSA and NaB resulted in the reductions of cleaved caspase 3, 6, 9 and PARP protein levels induced by H_2O_2, but reduction of such apoptotic proteins by TSA and NaB was abolished by pretreatment with MG132. MG132 alone in the absence of TSA and NaB did not change protein expression levels of cleaved caspases and PARP aforementioned. This indicates that the protective effects of HDAC inhibition in ESCs from oxidative stress were directly associated with the proteasome pathway.

HDAC INHIBITION FACILITATES CARDIAC COMMITMENT THAT DEPENDS ON THE PROTEASOME PATHWAY

We next sought to examine whether and how HDAC inhibition controls the facilitation of ESCs into cardiogenesis and, whether cardiac lineage commitments elicited by HDAC inhibition were determined by proteasome pathway. We detected ESC-derived cardiac lineage commitments during the EB growth. The culture protocol of ES, EB growth, and individual treatments are described in Figure 2A. As shown on the left panel of Figure 2A and supplementary Figure 3, ESC-derived cardiac structures stained with GATA4, MEF2C, and Nkx2.5 were reliably detected on day 14 EB; the levels of cardiac specific transcription factors positive-stained cells including GATA4, MEF2C, and Nkx2.5 in TSA or NaB treatment were $12.8 \pm 1.5\%$ and $14.7 \pm 1.9\%$ ($6.0 \pm 1.0\%$ in control); $16.1 \pm 1.1\%$ and $18.1 \pm 2.1\%$ ($9.0 \pm 1.5\%$ in control); and $13.4 \pm 1.2\%$ and $15 \pm 2.0\%$ ($6.7 \pm 1.2\%$ in control), respectively ($P < 0.05$ vs. control). In addition, the Western blot demonstrated that HDAC inhibition significantly increased protein expressions of alpha-actinin, alpha-SMA, GATA4, MEF2C, and Nkx2.5 as compared to the control group. The increased proteins were prevented by the administration of MG132 (Fig. 3 A and B). We next employed RT-PCR to analyze the transcriptional profiling of cardiac and smooth muscle genes. As compared to the control group, both TSA and NaB favored the increased mRNA expressions of α-actinin, α-SMA, GATA4, and MEF2C, whereas MG132 significantly mitigated the effect of HDAC inhibition on the mRNA expressions in cardiogenesis and angiogenesis (Fig. 3 C and D). Furthermore, using siRNA gene silencing and well-established in vitro cell culture model, we found that the specific knockdown of HDAC4 with HDAC4 siRNA exhibited the reduction of HDAC4 as compared to control-scrambled siRNA. Remarkably, genetic knockdown of HDAC 4 significantly enhanced mRNA expression in cardiogenesis and angiogenesis as described above, indicating the contribution of HDAC4 inhibition in the regulation of cardiogenesis (Supplementary Figure 4).

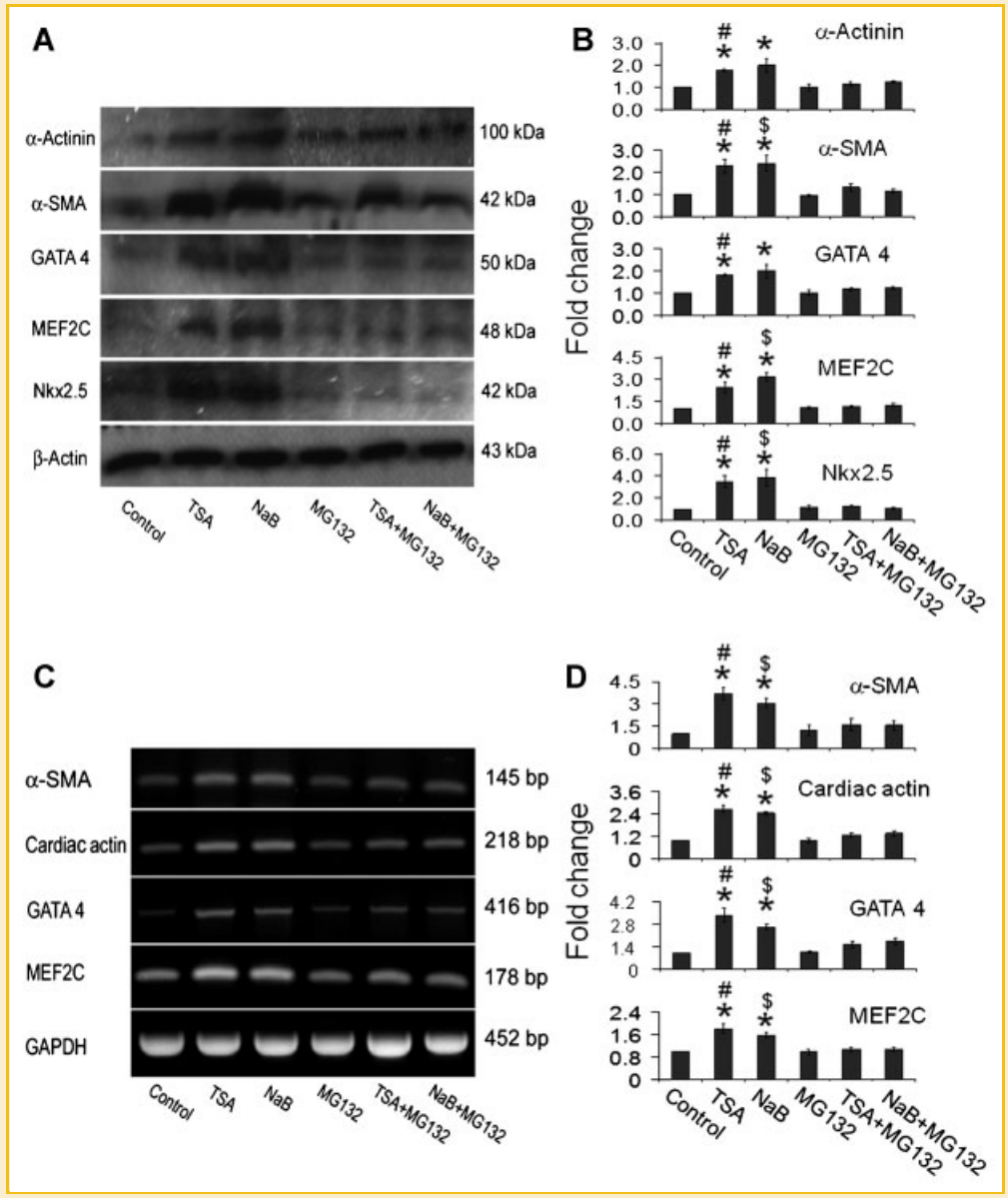

Fig. 3. Effect of HDAC inhibition on cardiac specific proteins and the transcriptional levels of cardiac gene: (A) Representative Western blot showing the effect of TSA, NaB, and MG132 on the contents of GATA4, MEF2C, Nkx2.5, cardiac actin, and α-smooth muscle actin (α-SMA). B: Quantification of GATA4, MEF2C, Nkx2.5, cardiac actin, and α-smooth muscle actin among individual groups(n = 3 per group); (C) representative DNA gel showing the effect of TSA, NaB, and MG132 on the contents of GATA4, MEF2C, NKX2.5, cardiac actin, and α-smooth muscle actin (α-SMA); (D) quantification of GATA4, MEF2C, Nkx2.5, cardiac actin, and α-smooth muscle actin among individual groups (n = 3 per group); values represent mean ± SEM; $^{*}P < 0.05$ versus control group, $^{\#}P < 0.05$ versus TSA + MG132 group, $^{\$}P < 0.05$ versus NaB + MG132 group.

THE PROTEASOME PATHWAY IMPACTS THE HDAC INHIBITION-STIMULATED EB GROWTH

We further assessed whether the proteasome pathway is involved in mediating the growth of EBs after HDAC inhibition following the initiation of the differentiation. We next monitored the growth of suspension EBs during differentiation. The diameters of suspension EBs were measured on days 8, 10, 12, and 14, respectively. EB diameters steadily increased in all of the groups. Although EB diameters were not found to be different on day 8 in all groups, HDAC inhibition with TSA and NaB preferentially stimulates EB growth on day 10, which was mitigated by treatment with MG132 (Fig. 4). Furthermore, HDAC inhibition led to the degradation of HDAC4 of differentiated ESC, which was blocked by treatment with MG132. We did not find the effect of HDAC inhibition on HDAC4 mRNA as compared to the control (Supplementary Figure 5). In addition, we found that TSA or NaB did not affect HDAC1, HDAC3, HDAC6, HDAC7 protein expressions (Supplementary Figure 6). Therefore, the results suggest the critical role of HDAC4 reduction in mediating EB growth in this study.

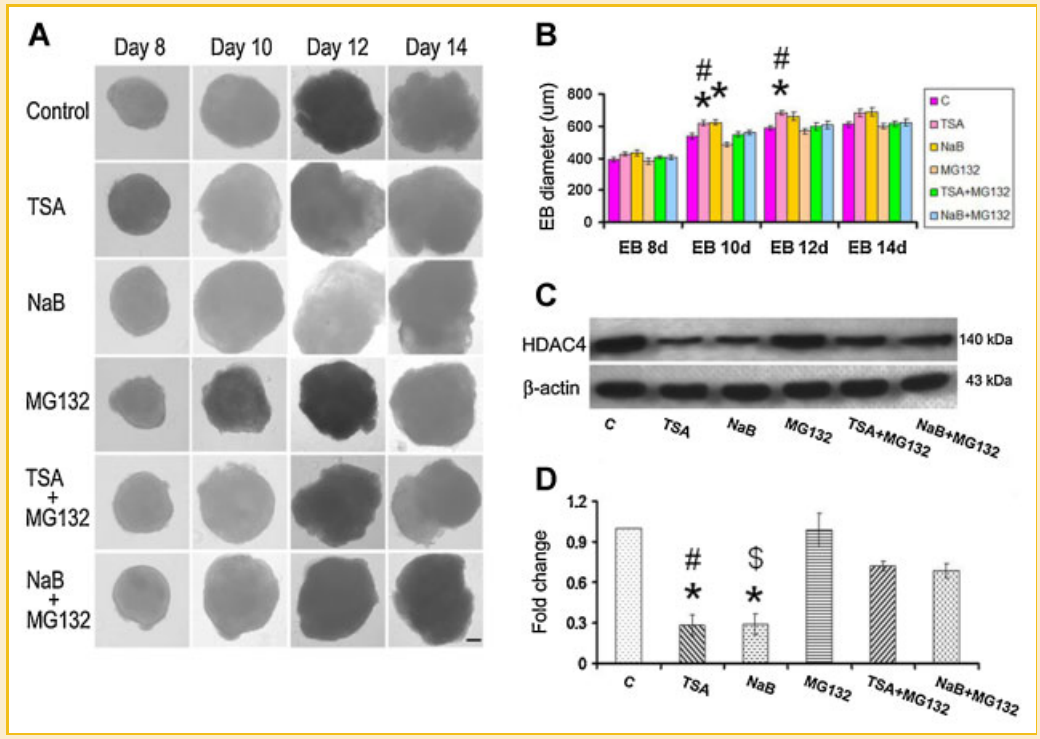

Fig. 4. Effect of HDAC inhibition on EB growth: (A) Representative image showing the growth of EB among the different treatments; Bar = 100 μm (B) quantification of EB diameters from growing EBs among individual groups (n = 6 per group); (C) representative Western blot showing HDAC4 protein levels on day 14 EBs; (D) quantification of HDAC4 protein levels (n = 3 per group); values represent mean ± SEM; $^{*}P < 0.05$ versus control group, $^{\#}P < 0.05$ versus TSA + MG132 group, $^{\$}P < 0.05$ versus NaB + MG132 group.

BLOCKADE OF PROTEASOME PATHWAY DEMONSTRATES DEFICIENCY OF ESC-DERIVED CARDIOMYOCYTES BY HDAC INHIBITION

To evaluate the effect of HDAC inhibition on the phenotype of ESC-derived myocytes, spontaneous rhythmic contractions were estimated starting from day 9 to day 14, and the beating rates of EBs within individual treatments were measured. During the differentiation stage, noticeable beating EBs appeared in all of the groups. Although the beating rate of EBs was approximately 20% in each group on day 9, the number of beating EBs significantly increased with the treatment of TSA or NaB from day 12 to day 14 as compared to the control group. Interestingly, MG132 blocked the beating percentage increase promoted by TSA and NaB (Fig. 5A). EB beating rates on day 14 are summarized in Figure 5B. The spontaneous beating rate is around 40% in the control group, rising to around 75% following treatment of HDAC inhibition. However, this increase in response to HDAC inhibition was inhibited by MG132, suggesting that HDAC inhibition promotes the formation of cardiac contracting EBs that involves the existence of proteasome system.

ACTIVATION OF MEF2 REQUIRES PROTEASOME PATHWAY IN THE DIFFERENTIATED ESCs

MEF2 is known to be crucial for directing the development of cardiogenesis. Activation of MEF2 will promote the cardiac lineages specification. The formation of HDAC4 with MEF2 complexes has been reported to repress MEF2 activity [Chan et al., 2003]. It is likely, but unknown, whether HDAC4 degradation will alleviate its inhibitory effect on MEF2, which subsequently acts as the determinant to affecting the formation of ESCs-derived myocytes. Since HDAC inhibitor treatments resulted in HDAC4 protein degradation, which was prevented by inhibition of proteasome, we next examined their effects on MEF2 reporter activity using the transient luciferase assays. As shown in Figure 6, inhibition of HDAC significantly increased the luciferase activity of 4×-MEF2-luc reporter construct, but an increase in MEF2 activity was abolished by MG132. These results demonstrate that inhibition of the proteasome in ESCs, which prevents HDAC4 degradation, reduces the activation of MEF2, supporting the notion that HDAC inhibition relying on the proteasome system precisely regulates activation of MEF2 that impact ESC-derived myocytes.

DISCUSSION

SALIENT FINDINGS

We have demonstrated that 1) HDAC inhibition increased the resistance of ESCs in response to oxidant stress, as indicated by an increase in ESC viability and decreases in cell death and apoptosis. These beneficial effects were mitigated by inhibition of proteasome system with MG132, suggesting that ESC survival is governed by HDAC inhibition and proteasome pathway; 2) HDAC inhibition facilitated the lineage restriction of cardiogenesis and angiogenesis, as evidenced by increases in the expression of transcriptional

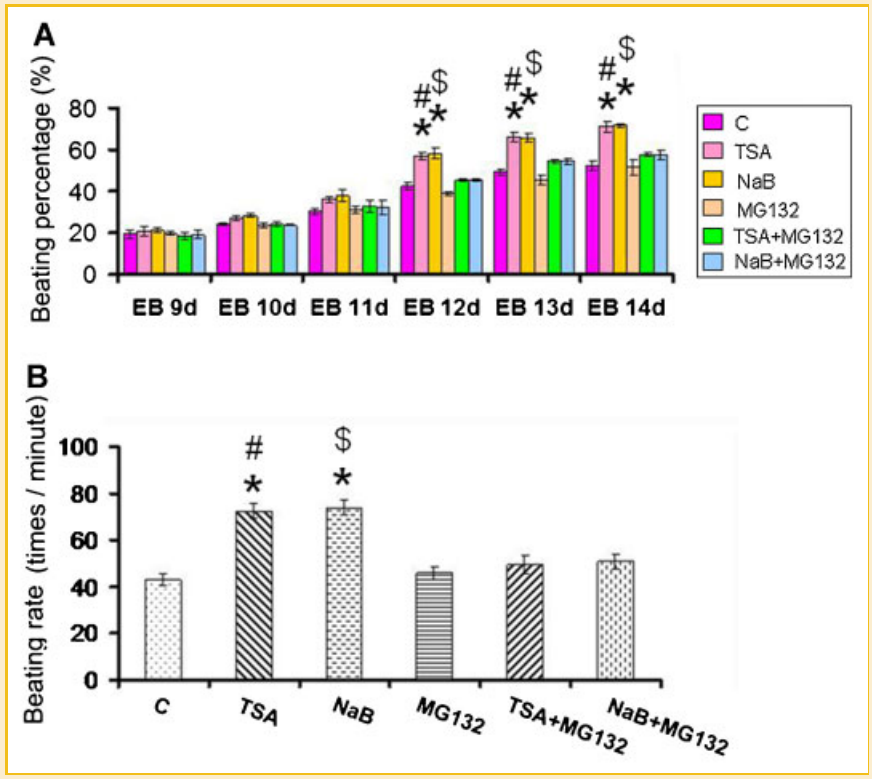

Fig. 5. Effect of HDAC inhibition on the spontaneous rhythmic contracting EB: (A) Percentage of Beating EBs among the different groups (n = 3 per group); (B) quantification of EB beating rate among the groups (n = 8 per group); values represent mean ± SEM; $^{*}P < 0.05$ versus control group, $^{\#}P < 0.05$ versus TSA + MG132 group, $^{\$}P < 0.05$ versus NaB + MG132 group.

cardiac and angiogenic genes. These were closely associated with a remarkable increase in EB growth as well as spontaneous rhythmic contractions, which were blocked with MG132, supporting the notion that HDAC inhibition co-ordinates with the proteasome system to control ESC specification; 3) HDAC inhibition specifically led to HDAC4 degradation in ESCs in addition to inhibiting its activity, whereas blockade of the proteasome pathway reversed this process, which implicates the importance of HDAC4 degradaton in regulating ESC lineage commitments; 4) HDAC inhibition resulted in activation of MEF2 during the differentiation of ESCs, which requires a functional proteasome pathway, pointing out that HDAC inhibition/proteasome system and MEF2 constitute a unique cascade in directing the lineage decision and survival of ESCs. Taken together, this study is the first to demonstrate that HDAC inhibition and the proteasome pathway plays a crucial role in mediating ESCs to commit cardiogenesis, angiogenesis, and cell survival.

There is plenty of experimental evidence stating that most ESC-derived cardiomyocytes initially die soon after transplantation into the infarcted myocardium. One of the major reasons for this is the vulnerability of ESCs to oxidant stress [Rota et al., 2006]. Given that we identified the abundant expression of HDAC4 in ESCs, we first attempted to examine whether HDAC inhibition could increase the resistance of ESCs to oxidant stress using in vitro cultured ESCs from our previous studies [Tseng et al., 2010; Zhang et al., 2010]. Treatment of ESCs with HDAC inhibitors augmented resistance to

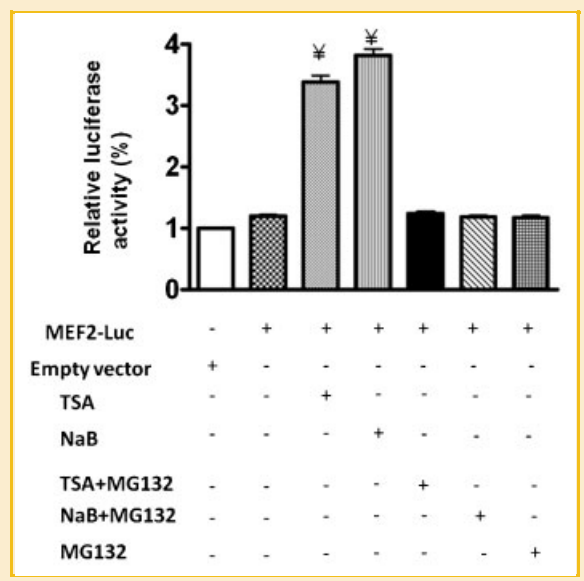

Fig. 6. Activities of luciferase were used to assess the MEF2 transcriptional activity by HDAC inhibitors with or without proteasome inhibitor. ESCs were transiently transfected with the MEF2-luciferase reporter construct (4X-MEF2-luc) luciferase reporter construct. Twenty-four hours after transfection, cells were treated with or without TSA or NaB and luciferase activities were determined and results were normalized to the basal levels (empty vector). Results are mean ± SE (n = 5/group), $^{¥}P < 0.001$ versus empty vector, MEF2-luc, TSA + MG132, NaB + MG132, and MG132.

oxidant stress by enhancing cell viability and decreasing cell death, both of which are associated with the reduction of apoptotic cell numbers. In this study, we demonstrated that HDAC inhibition suppressed the expression of cleaved caspases and PARP, which might represent an event associated with the inhibition of apoptosis. The direct target of HDAC4 inhibition that constitutes major pathway to activate the apoptosis remains unclear. Also, it is interesting to evaluate whether anti-apoptotic effects of HDAC inhibition contributes to cardiac commitments. Strikingly, these protective effects elicited by HDAC inhibitors were totally diminished in ESCs treated with proteasome inhibitor MG132. This suggests the requirement of the proteasome system for HDAC inhibition to protect ESCs from oxidant injury. It is supported by our recent observation that HDAC inhibition played a primary role in reducing cellular injury of embryonic H9C2 cell and ischemic hearts [Zhang et al., 2010].

It is known that development and cell fate determination require genetic and epigenetic co-ordination. As a naïve cell differentiates toward a particular lineage, modifications of the chromatin occur to activate lineage-specific genes and silence "stemness" genes and those associated with alternative cell fates [Song et al., 2006]. The most striking example shown here is that small molecules and HDAC inhibitors increase the reprogramming efficiency of human fibroblasts into iPS and ESC self-renewal across species [Ware et al., 2009]. Our intriguing evidence here shows that the formation of EB in the presence of both trichostatin A and sodium butyrate was noticeably larger than the control group, but this effect of HDAC inhibition disappeared in the presence of the proteasome inhibitor. Furthermore, the effect of HDAC inhibition on ESC-derived cardiac lineage comments was eliminated by MG132, addressing the indispensible function of the proteasome system in initiating ESC lineage specification. Although we demonstrated that trichostatin A and sodium butyrate effectively inhibited HDAC activity, HDAC4 degradation displayed after HDAC inhibition was reversed in the presence of the proteasome inhibitor, implying that the proteasome system preferentially targets this specific HDAC isoform and led to HDAC4 degradation in ESCs. The mechanism that directs degradation of HDAC4 in ESCs after HDAC inhibition remains to be determined. It is tempting to speculate that post-modification of HDACs serves as a signal for ubiquitination or poly-sumoylation. Identification of these signals regulating HDAC4 degradation after HDAC inhibition in ESCs is currently under investigation. MEF2 protein interacts with HDAC4, resulting in the repression of MEF2-dependent genes [McKinsey et al., 2000], whereas genetic deletion of MEF2 resulted in embryonic lethal death [Lin et al., 1997]. Evidence from these transgenic animal studies illustrates that class II HDACs are associated with MEF2 and negatively regulate the development of cardiogenesis. Interestingly, increased transcriptional activity of MEF2 of HDAC inhibition was repressed by proteasome inhibitors, emphasizing the co-ordination between HDAC and the proteasome pathway in mediating cardiac commitments of ESCs directly through MEF2. Additionally, we have recently demonstrated that HDAC inhibition enhanced histone 4 acetylation in myocytes. It is also interesting to elucidate whether HDAC inhibition interacts with the proteasome pathway to impact epigenetic regulation to modulate ESC specification and survival, which will provide additional important information for understanding its mechanism.

CONCLUSION

In this study, we demonstrated that HDAC inhibition increased the resistance of ESCs to oxidant stress, as indicated by the reduction of cell death, the increase in the cell viability, the decreases in apoptosis. These effects disappeared in the presence of proteasome inhibition. Furthermore, both trichostatin A and sodium butyrate triggered the degradation of HDAC4, which was reversed by MG132, suggesting that the proteasome system determines HDAC4 degradation after HDAC inhibition. On the other hand, HDAC inhibition did not significantly change the expressions of other HDAC isoforms, suggesting that HDAC4 may play a major role in determining the cardiogenesis. Notably, trichostatin A and sodium butyrate stimulate the growth of EBs, which are closely associated with a faster spontaneous rhythmic contraction, a cardiac lineage commitment, increased up-regulation of cardiac actin, and cardiac specific transcriptional factors, which were abolished by MG132. Finally, HDAC inhibition-induced increase in cardiac transcriptional factor, MEF2 activity, was repressed by the inhibition of proteasome. Taken together, HDAC inhibition coordination with the proteasome pathway constitutes a major cascade in controlling cardiogenesis and promoting the survival of ESCs.

ACKNOWLEDGMENTS

The work is supported by the National Heart, Lung, and Blood Institute Grant (R01 HL089405) and American Heart Association-National center (0735458N) to TCZ.

REFERENCES

Chan JK, Sun L, Yang XJ, Zhu G, Wu Z. 2003. Functional characterization of an amino-terminal region of HDAC4 that possesses MEF2 binding and transcriptional repressive activity. J Biol Chem 278(26):23515–23521.

Cheung P, Allis CD, Sassone-Corsi P. 2000. Signaling to chromatin through histone modifications. Cell 103:263–267.

Dovey OM, Foster CT, Cowley SM. 2010. Histone deacetylase 1 (HDAC1), but not HDAC2, controls embryonic stem cell differentiation. Proc Natl Acad Sci USA 107(18):8242–8247.

Fischle W, Emiliani S, Hendzel MJ, Nagase T, Nomura N, Voelter W, Verdin E. 1999. A new family of human histone deacetylases related to Saccharomyces cerevisiae HDA1. Biol Chem 274:11713–11720.

Foster CT, Dovey OM, Lezina L, Luo JL, Gant TW, Barlev N, Bradley A, Cowley SM. 2010. Lysine-specific demethylase 1 regulates the embryonic transcriptome and CoREST stability. Mol Cell Biol 30(20):4851–4863.

Grozinger CM, Hassig CA, Schreiber SL. 1999. Three proteins define a class of human histone deacetylases related to yeast Hda1p. Proc Natl Acad Sci USA 96:4868–4873.

Hansen JC, Tse C, Wolffe AP. 1998. Structure and function of the core histone N-termini: More than meets the eye. Biochemistry 37:17637–17641.

Hassig CA, Tong JK, Fleischer TC, Owa T, Grable PG, Ayer DE, Schreiber SL. 1998. A role for histone deacetylase activity in HDAC1-mediated transcriptional repression. Proc Natl Acad Sci USA 95:3519–3524.

Huangfu D, Osafune K, Maehr R, Guo W, Eijkelenboom A, Chen S, Muhlestein W, Melton DA. 2008. Induction of pluripotent stem cells from primary human fibroblasts with only Oct4 and Sox2. Nat Biotechnol 26(11):1269–1275.

Kee HJ, Sohn IS, Nam KI, Park JE, Yin Z, Ahn Y, Jeong MH, Bang YJ, Kim N, Kim JK, Kim KK, Epstein JA, Kook H. 2006. Inhibition of histone deacetylation blocks cardiac hypertrophy induced by angiotensin II infusion and aortic banding. Circulation 113:51–59.

Kong Y, Tannous P, Lu G, Berenji K, Rothermel BA, Olson EN, Hill JA. 2006. Suppression of class I and II histone deacetylases blunts pressure-overload cardiac hypertrophy. Circulation 113:2579–2588.

Lagger M, O'Carroll D, Rembold M, Khier H, Tischler J, Weitzer G, Schuettengruber B, Hauser C, Brunmeir R, Jenuwein T, Seiser C. 2002. Essential function of histone deacetylase 1 in proliferation control and CDK inhibitor repression. EMBO J 21(11):2672–2681.

Lin Q, Schwarz J, Bucana C, Olson EN. 1997. Control of mouse cardiac morphogenesis and myogenesis by transcription factor MEF2C. Science 276(5317):1404–1407.

Luger K, Mader AW, Richmond RK, Sargent DF, Richmond TJ. 1997. Crystal structure of the nucleosome core particle at 2.8 A resolution. Nature 389:251–260.

Maltsev VA, Wobus AM, Rohwedel J, Bader M, Hescheler J. 1994. Cardiomyocytes differentiated in vitro from embryonic stem cells developmentally express cardiac-specific genes and ionic currents. Circ Res 75(2):233–244.

McKinsey TA, Zhang CL, Lu J, Olson EN. 2000. Signal-dependent nuclear export of a histone deacetylase regulates muscle differentiation. Nature 408(6808):106–111.

Moresi V, Williams AH, Meadows E, Flynn JM, Potthoff MJ, McAnally J, Shelton JM, Backs J, Klein WH, Richardson JA, Bassel-Duby R, Olson EN. 2010. Myogenin and class II HDACs control neurogenic muscle atrophy by inducing E3 ubiquitin ligases. Cell 143(1):35–45.

Potthoff MJ, Wu H, Arnold MA, Shelton JM, Backs J, McAnally J, Richardson JA, Bassel-Duby R, Olson EN. 2007. Histone deacetylase degradation and MEF2 activation promote the formation of slow-twitch myofibers. J Clin Invest 117(9):2459–2467.

Rota M, LeCapitaine N, Hosoda T, Boni A, De Angelis A, Padin-Iruegas ME, Esposito G, Vitale S, Urbanek K, Casarsa C, Giorgio M, Lüscher TF, Pelicci PG, Anversa P, Leri A, Kajstura J. 2006. Diabetes promotes cardiac stem cell aging and heart failure, which are prevented by deletion of the p66shc gene. Circ Res 99(1):42–52.

Rusty LM, Christopher AD, Matthew JP, Michael H, Jens F, Xiaoxia Q, Joseph AH, James AR, Eric NO. 2007. Histone deacetylases 1 and 2 redundantly regulate cardiac morphogenesis, growth, and contractility. Genes Dev 21(14): 1790–1802.

Smith AG. 2001. Embryo-derived stem cells: Of mice and men. Annu Rev Cell Dev Biol 17:435–462.

Song K, Backs J, McAnally J, Qi X, Gerard RD, Richardson JA, Hill JA, Bassel-Duby R, Olson EN. 2006. The transcriptional coactivator CAMTA2 stimulates cardiac growth by opposing class II histone deacetylases. Cell 125(3):453–466.

Strahl BD, Allis CD. 2000. The language of covalent histone modifications. Nature 403:41–45.

Su H, Wang X. 2010. The ubiquitin-proteasome system in cardiac proteinopathy: A quality control perspective. Cardiovasc Res 85(2):253–262.

Tamaki T, Akatsuka A, Okada Y, Uchiyama Y, Tono K, Wada M, Hoshi A, Iwaguro H, Iwasaki H, Oyamada A, Asahara T. 2008. Cardiomyocyte formation by skeletal muscle-derived multi-myogenic stem cells after transplantation into infarcted myocardium. PLoS One 3(3):e1789.

Thomson JA, Itskovitz-Eldor J, Shapiro SS, Waknitz MA, Swiergiel JJ, Marshall VS, Jones JM. 1998. Embryonic stem cell lines derived from human blastocysts. Science 282(5391):1145–1147.

Trivedi CM, Luo Y, Yin Z, Zhang M, Zhu W, Wang T, Floss T, Goettlicher M, Noppinger PR, Wurst W, Ferrari VA, Abrams CS, Gruber PJ, Epstein JA. 2007. Hdac2 regulates the cardiac hypertrophic response by modulating Gsk3 beta activity. Nat Med 13(3):324–331.

Tseng A, Stabila J, McGonnigal B, Yano N, Yang MJ, Tseng YT, Davol PA, Lum LG, Padbury JF, Zhao TC. 2010. Effect of disruption of Akt-1 of lin(-)c-kit(+) stem cells on myocardial performance in infarcted heart. Cardiovasc Res 87(4):704–712.

Turner BM. 2000. Histone acetylation and an epigenetic code. Bioessays 22:836–845.

Verdin E, Dequiedt F, Kasler HG. 2003. Class II histone deacetylases: Versatile regulators. TRENDS in Genetics 19:286–293.

Vigushi DM, Coombes RC. 2004. Targeted histone deacetylase inhibition for cancer therapy. Curr Cancer Targ 4:205–218.

Wang AH, Bertos NR, Vezmar M, Pelletier N, Crosato M, Heng HH, Th'ng J, Han J, Yang XJ. 1999. HDAC4, a human histone deacetylase related to yeast HDA1, is a transcriptional corepressor. Mol Cell Biol 19:7816–7827.

Ware CB, Wang L, Mecham BH, Shen L, Nelson AM, Bar M, Lamba DA, Dauphin DS, Buckingham B, Askari B, Lim R, Tewari M, Gartler SM, Issa JP, Pavlidis P, Duan Z, Blau CA. 2009. Histone deacetylase inhibition elicits an evolutionarily conserved self-renewal program in embryonic stem cells. Cell Stem Cell 4(4):359–369.

Yuan X, Wan H, Zhao X, Zhu S, Zhou Q, Ding S. 2011. Combined chemical treatment enables Oct4-induced reprogramming from mouse embryonic fibroblasts. Stem Cells 29(3):549–553.

Zhang CL, McKinsey TA, Chang S, Antos CL, Hill JA, Olson EN. 2002. Class II histone deacetylases act as signal-responsive repressors of cardiac hypertrophy. Cell 110(4):479–488.

Zhang LX, Zhao Y, Cheng G, Guo TL, Chin YE, Liu PY, Zhao TC. 2010. Targeted deletion of NF-kappaB p50 diminishes the cardioprotection of histone deacetylase inhibition. Am J Physiol Heart Circ Physiol 298(6): H2154–H2163.

Zhao TC, Taher MM, Valerie KC, Kukreja RC. 2001. p38 Triggers late preconditioning elicited by anisomycin in heart: Involvement of NF-kappaB and iNOS. Circ Res 89(10):915–922.

Zhao TC, Cheng G, Zhang LX, Tseng YT, Padbury JF. 2007. Inhibition of histone deacetylases triggers pharmacologic preconditioning effects against myocardial ischemic injury. Cardiovasc Res 76:473–481.